Mar Syst Ocean Technol (2017) 12:252–261
DOI 10.1007/s40868-017-0038-y

Transient point load induced response of Kirchhoff's plate with translationally constrained edges: aircraft landing on floating airports

N. Datta[1] · **J. D. Thekinen**[2]

Received: 30 May 2017 / Accepted: 29 August 2017 / Published online: 5 September 2017

Abstract Dynamic analysis of thin rectangular elastically supported plates to transient loads is presented. A floating airport is modeled as a horizontal Kirchhoff's plate, which is elastically supported at the ends, and is subjected to the impact of aircrafts landing and deceleration over its length. This sets the free–free–free–free plate into high-frequency vibration, causing flexural stress waves to travel over the plate. First, the beam natural frequencies and modeshapes in either direction are generated with these complexities. The eigenvalue analysis of the governing differential equation is done, using the weighted summation of the product of the beam modes. The radiation pressure on the bottom side of the plate is included to reduce the frequencies by the added-mass effect. The plate is then subjected to decelerating shock loads. The vibratory response is analyzed by the computationally efficient normal mode analysis. The amplification factor versus the taxiing time of the moving load is generated. This gives insights into the maximum stress encountered under the transient load, as function of taxiing time and support.

Keywords Plate vibration · Free edge · Shock loads · Normal mode analysis · Added mass

List of symbols

L	Length of the plate
B	Width of the plate
h	Thickness of the plate
ρ	Density of the beam material
ρ_{water}	Density of water
ρ_{material}	Density of plate material
E	Elastic modulus of the material
I	Second moment of area of the cross section of the beam about the horizontal neutral axis
x	Space variable along x-direction
y	Space variable along y-direction
t	Time variable
$\phi_j(x)$	jth beam modeshape in the x-direction
$\phi_l(y)$	lth beam modeshape in the y-direction
$\Phi_k(x, y)$	kth plate modeshape
$q_j(t)$	Principal coordinate
$\Psi(x, y, z, t)$	Velocity potential of the fluid
Ψ_k	kth velocity potential of the fluid
Ψ_k^*	kth velocity potential of the fluid per unit velocity of the kth principal coordinate
A_{kn}	kth generalized added mass under the nth plate modeshapes
$F(x, y, t)$	Transient load
ω_{n1}	Fundamental natural frequency of the plate
T_{n1}	Fundamental natural period of the plate
$z(x, y, t)$	Dynamic flexural deflection of the plate
$z_{\text{st}}(x, y, t)$	Static flexural deflection of the plate

1 Introduction

The increasing world population has been congesting inhabitable land for the last few decades. Smaller and island countries (e.g., Japan) have been foraying into floating cities and airports, and thus, the design of such VLFS (very large floating structure) has been gaining relevance. Floating airports are subject to impact and transient

✉ N. Datta
ndatta@naval.iitkgp.ernet.in

[1] Department of Ocean Engineering and Naval Architecture, Indian Institute of Technology, Kharagpur, India

[2] Department of Mechanical Engineering, Purdue University, West Lafayatte, USA

loads of the taxiing aircraft. The transient force sets the plate in vibrations, exciting all its natural frequencies to various amplitudes. This causes dynamic deflections and stresses in the VLFS, which must be analyzed to ensure a sound structural design.

Robinson and Palmer [1] theoretically formulated the frequency parameter of a Free–Free–Free–Free (FFFF) plate in contact with water on one side, stopping short of calculating the frequencies and modeshapes. Kagemoto et al. [2] calculated the wave-response of a VLFS using substructure models using FEA, and experimentally. This work did not take any shock loads into account. It studied only one case of plate size and configuration, but could not generalize the frequencies, modeshapes, added masses, and dynamic loading factors. Endo [3] used FEA to study the VLFS response due to aircraft landing/takeoff. Seto et al. [4] studied the two-way coupled Mega-Float vibratory response due to wave action. Hashemi et al. [5] studied the free vibration of elastically supported plates with water on one side, using the Ritz method.

None of the above literature studied the impact-induced vibration of elastically supported plates, in contact with water on one side, due to aircraft landing, using a semi-analytical approach. In this work, a floating airport is modeled as a rectangular plate with water on one side, supported on the edges by elastic supports. The sea is assumed to be calm. The structure is assumed to be very lightly damped. First, the free (dry) vibration analysis of the plate is done using the Galerkin's method, generating the dry natural frequencies and modeshapes. The radiation pressure has been included with the source distribution technique, leading to added masses associated with each modeshape and the corresponding reduced (wet) natural frequencies. This is followed by a forced vibration analysis of the plate, due to the impact of the landing aircraft, which decelerates to zero velocity. The dynamic analysis is done with the normal mode summation method. The corresponding static analysis is done by the Galerkin's method. The global maximum dynamic deflection is normalized by the global maximum static deflection to generate the dynamic loading factor (DLF) for various taxiing time and decelerations. Impact and transient loads cause the participation of the higher-order modes. Optimized taxiing duration and decelerations has been recommended, which leads to the minimum dynamic deflections and stresses.

2 Problem formulation

The floating airport is modeled as a horizontal Kirchhoff's plate (Fig. 1; Table 1), of length L, width B, thickness h, flexural rigidity D, floating over water of density ρ_{water}, and supported over its edges by vertical elastic supports of spring constant k. The radiation damping is assumed to be zero, i.e., radiation pressure is almost nearly in phase with the vertical acceleration of the body. The transient force (Table 2) is modeled as a Heaviside step function with an initial velocity $'u'$ m/s along L, and decelerated to zero velocity, over a taxiing distance $'S' = ut - \frac{1}{2}at_{\text{tax}}^2$, and for a taxiing duration of t_{tax}. The deceleration $'a' = \frac{u^2}{2S}\text{m/s}^2$.

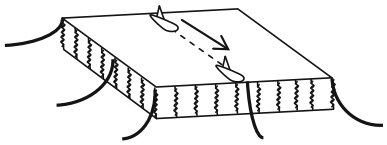

Fig. 1 Elastically supported plate

Table 1 Plate parameters

Plate	Symbol	Unit
Length	L	m
Breadth	B	m
Thickness	h	m
Flexural rigidity	D	Nm
Density of water	ρ_{water}	kg/m^3
Edge spring constant	k	N/m

3 Analysis methodology

The cross-sectional view of the floating airport, at $y = B/2$, is shown in Fig. 2. The aircraft lands at position A, with an initial horizontal velocity $'u'$ m/s, and decelerates to rest at position B. The vertical velocity of the craft is assumed to be nearly zero, and there is no vertical impact on the plate due to the landing. The plate vibration modeshape $\Phi_k(x, y)$ is assumed to be a weighted superposition of the product of the beam modeshapes $\phi_j(x)$ and $\phi_l(y)$ in either direction. The beam modeshapes with elastically restrained edges need to be first established, which will later act as admissible functions into the plate vibration analysis.

Table 2 Taxiing parameters

Aircraft landing	Symbol	Unit
Initial velocity of the aircraft	u	m/s
Final velocity of the aircraft	0	m/s
Taxiing time	t_{tax}	s
Taxiing distance	S	m
Deceleration	a	m/s^2
Transient force	F	N

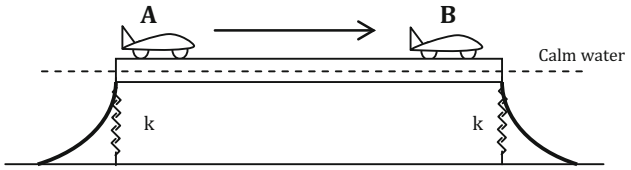

Fig. 2 Elastically supported beam

The governing differential equation (GDE) of free vibration of an elastically supported beam is given as follows:

$$m\frac{\partial^2 z(x,t)}{\partial t^2} + EI\frac{\partial^4 z(x,t)}{\partial x^4} = 0 \tag{1}$$

Equation (1) is subject to the boundary conditions:

$$z''(0) = z''(L) = 0; EIz'''(0) = -kz(0), EIz'''(L) = -kz(L), \tag{2a–d}$$

i.e., the end bending moment is zero, while the shear force at the ends balances the spring force due to the end deflection. In Eq. (2(a–d)), as $k \to 0$, it behaves like a Free–Free (FF) beam; while as $k \to \infty$, it behaves as a simply supported (SS) beam. The dynamic deflection is expressed as $z(x,t) = G(x)F(t)$. Using the method of separation of variables, the spatial component is $G^{\mathrm{IV}}(x) = \frac{m\omega^2}{EI}G(x) \Rightarrow G^{\mathrm{IV}}(x) = \beta^4 G(x)$; whose general solution is

$$G(x) = G_1\cos\beta x + G_2\sin\beta x + G_3\cosh\beta x + G_4\sinh\beta x. \tag{3}$$

The constants $G1, G2, G3, G4$ in Eq. (3) are calculated from the boundary conditions (Eq. 2(a–d)):

$$\begin{aligned}
&-G_1 + G_3 = 0; -G_1\cos\beta L - G_2\sin\beta L + G_3\cosh\beta L \\
&\qquad + G_4\sinh\beta L \\
&\qquad = 0; \frac{k}{EI}G_1 + \beta^3 G_2 + \frac{k}{EI}G_3 - \beta^3 G_4 = 0; \\
&\left(\frac{k}{EI}\cos\beta L - \beta^3\sin\beta L\right)G_1 + \left(\frac{k}{EI}\sin\beta L + \beta^3\cos\beta L\right)G_2 \\
&+ \left(\frac{k}{EI}\cosh\beta L - \beta^3\sinh\beta L\right)G_3 \\
&+ \left(\frac{k}{EI}\sinh\beta L - \beta^3\cosh\beta L\right)G_4 \\
&= 0.
\end{aligned} \tag{4a–d}$$

Writing the above system of Eq. (4(a–d)) in the matrix form and equating the determinant to zero (non-trivial solution) generate the frequency equation, which is a transcendental equation, satisfied by an infinite number of unique values βL, each corresponding to a natural frequency. The eigenvectors of Eq. (4(a–d)) generate the constants $G1, G2, G3, G4$, and thus $\phi_j(x)$.

3.1 Dry free vibration of the plate

The GDE of free vibration of an elastically supported Kirchhoff's plate is expressed as follows:

$$m\frac{\partial^2 z(x,y,t)}{\partial t^2} + D\left(\frac{\partial^4 z(x,y,t)}{\partial x^4} + \frac{\partial^4 z(x,y,t)}{\partial x^2\partial y^2} + \frac{\partial^4 z(x,y,t)}{\partial y^4}\right) = 0. \tag{5}$$

The bending moments M_x and M_y are zero at the ends, and the shear force at the edges equals the spring force produced due to the edge deflection. As $k \to 0$, the plate behaves like a FFFF plate, while as $k \to \infty$, it behaves as a simply supported (SSSS) plate. The total out-of-plane dynamic deflection in Eq. (5) is $z(x, y, t)$. Separating the variables of Eq. (5), we assume $\Phi_k(x, y)$ as the kth spatial shape function, and $q_k(t)$ as the temporal function of the kth vibratory mode. The dynamic deflection of the plate is approximately

$$z(x,y,t) = \sum_{k=1}^{\infty}\Phi_k(x,y)q_k(t) \tag{6}$$

with the 3-D plate modeshape in Eq. (6) defined as

$$\begin{aligned}
\Phi_k(x,y) &= \sum_{j=1}^{\mathrm{modex}}\sum_{l=1}^{\mathrm{modey}} A_{jl}^k\phi_j(x)\phi_l(y) \\
&= \sum_{j=1}^{\mathrm{modex}}\sum_{l=1}^{\mathrm{modey}} A_{jl}^k G_{jl}, \text{ i.e., } G_{jl}(x,y) = \phi_j(x)\phi_l(y)
\end{aligned} \tag{7}$$

mode x is the number of modes considered in the x-direction, mode y is the number of modes considered in the y-direction, and $\phi_j(x)$ and $\phi_l(y)$, are the respective 2-D beam modeshapes (orthogonal set of functions). A_{jl}^k is the amplitude of each $G_{ij}(x,y)$ for the kth natural frequency of vibration (Eq. 7). The natural frequency ω_n is non-dimensionalized by the factor $\sqrt{\frac{D}{\rho_{\mathrm{material}}hL^2B^2}}$.

3.2 Plate vibration with water on one side

The 3-D boundary value problem of wet vibration of plates, with water on one side, is framed as shown in Fig. 3. The flexible plate has a semi-infinite fluid domain on one side, the other side being dry. Sides DA and BC are formed by the high-frequency limit of the combined free surface

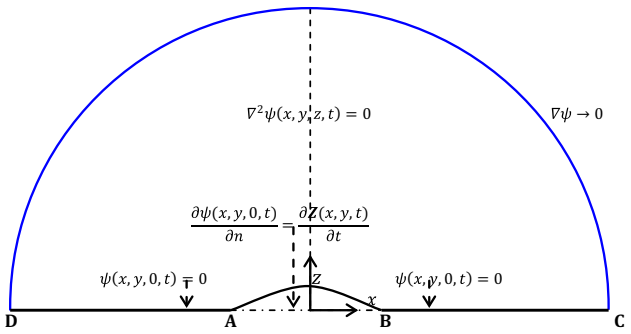

Fig. 3 Boundary value problem

boundary condition (Dirichlet condition). AB represents the plate. Assuming inviscid, incompressible, irrotational flow, the velocity potential satisfies the Laplace equation, i.e., $\nabla^2\psi(x,y,z,t)=0$, subject to the boundary conditions:

(a) the velocity potential on DA and BC are zero (high-frequency limit of free surface water wave), i.e., $\psi(x,\,y,\,0,\,t)=0$
(b) the normal fluid velocity on AB equals the structural velocity, i.e., $\frac{\partial\psi(x,y,0,t)}{\partial n}=\frac{\partial Z(x,y,t)}{\partial t}$
(c) fluid velocity tends to zero at the far-field, i.e., $\nabla\psi\to 0$.

The governing differential equation for the free wet vibration of a Kirchhoff's plate, using Eq. (6), is

$$\begin{aligned}&\sum_{k=1}^{\infty} m\Phi_k(x,y)\frac{\mathrm{d}^2q_k(t)}{\mathrm{d}t^2}+\sum_{k=1}^{\infty}D\nabla^4\Phi_k(x,y)q_k(t)\\&=\rho_{\text{water}}\sum_{k=1}^{\infty}\Psi_k^*(x,y,0)\frac{\mathrm{d}^2q_k(t)}{\mathrm{d}t^2}\\&\Rightarrow\sum_{k=1}^{\infty}\left[m+\rho_{\text{water}}\left\{\int_S 2\Phi_k(\xi,\eta)G_{\text{PQ}}\mathrm{d}S_{\text{Q}}\right\}\right]\Phi_k(x,y)\frac{\mathrm{d}^2q_k(t)}{\mathrm{d}t^2}\\&\quad+\sum_{k=1}^{\infty}D\nabla^4\Phi_k(x,y)q_k(t)\\&=0\end{aligned}\tag{8}$$

In Eq. (8), Ψ_k^* is the kth radiation velocity potential per unit velocity of the principal coordinate $\frac{\mathrm{d}q_k(t)}{\mathrm{d}t}$. It can be related to the 3-D Green's function G_{PQ}, where P is the field point and Q is the source point. The body-boundary condition of no-penetration relates it to the plate mode-shape. The details are found in Datta [6], and Datta and Troesch [8]. Pre-multiplying Eq. (8) by the rth plate modeshape $\Phi_r(x,y)$ and integrating over the surface area of the plate gives the generalized mass, generalized added mass, and generalized stiffness.

$$\begin{aligned}&\sum_{k=1}^{\infty}\left[\int_0^L\int_0^B\Phi_k(x,y)m\Phi_n(x,y)\mathrm{d}x\mathrm{d}y\right]\frac{\mathrm{d}^2q_k(t)}{\mathrm{d}t^2}\\&+\sum_{k=1}^{\infty}\left[\int_0^L\int_0^B\Phi_k(x,y)\rho_{\text{water}}\Psi_k^*(x,y,0)\mathrm{d}x\mathrm{d}y\right]\frac{\mathrm{d}^2q_k(t)}{\mathrm{d}t^2}\\&+\sum_{k=1}^{\infty}\left[\int_0^L\int_0^B\Phi_k(x,y)D\nabla^4\Phi_n(x,y)\mathrm{d}x\mathrm{d}y\right]q_k(t)\\&=0\Rightarrow\sum_{n=1}^{k}(M_{kn}+A_{kn})\ddot{q}_n(t)+\sum_{n=1}^{k}K_{kn}q_n(t)=0\end{aligned}\tag{9}$$

with generalized added mass is given as

$$A_{kn}=\int_0^L\int_0^B\Phi_k(x,y)\rho_{\text{water}}\Psi_k^*(x,y,0)\mathrm{d}x\mathrm{d}y.\tag{10}$$

The non-dimensional added virtual mass increment (NAVMI) factor depends only on the modeshape. It is given as

$$\text{NAVMI}=\frac{\int_0^L\int_0^B\Phi_k(x,y)\Psi_k^*(x,y)\mathrm{d}x\mathrm{d}y}{\int_0^L\int_0^B\Phi_k(x,y)\Phi_n(x,y)\mathrm{d}x\mathrm{d}y}.\tag{11}$$

3.3 Plate vibration under transient force

The governing differential equation for forced vibration of an elastically supported plate under a moving point load is given as

$$\begin{aligned}&m\frac{\partial^2z(x,y,t)}{\partial t^2}+D\left(\frac{\partial^4z(x,y,t)}{\partial x^4}+\frac{\partial^4z(x,y,t)}{\partial x^2\partial y^2}+\frac{\partial^4z(x,y,t)}{\partial y^4}\right)\\&=F\delta\left(x-ut+\frac{1}{2}at^2\right).\end{aligned}\tag{12}$$

Equation (12) is solved by the normal mode summation method. Substitution of Eq. (6) above, and integration with weighting functions over the space, gives the normal mode expansion of the governing differential equation as a function of time only, as

$$\begin{aligned}&\sum_{n=1}^{\infty}M_{kn}\ddot{q}_n(t)+\sum_{n=1}^{\infty}K_{km}q_n(t)=gf_k(t)\\&\qquad\Rightarrow\ [M]\{\ddot{q}(t)\}+[K]\{q(t)\}\\&\qquad=\{gf(t)\},\end{aligned}\tag{13}$$

where Generalized mass $\equiv M_{kn}=\int_0^L\int_0^B\Phi_k(x,y)m\Phi_n(x,y)$ $\mathrm{d}x\mathrm{d}y$, Generalized stiffness $\equiv K_{kn}=\int_0^L\int_0^B\Phi_k(x,y)\ D\nabla^4\Phi_n$

$(x,y)\mathrm{d}x\mathrm{d}y$, Generalized forcing $\equiv gf_k = \int_0^L \int_0^B \Phi_k(x,y) F(x,y,t)\mathrm{d}x\mathrm{d}y$. Equation (13) is solved numerically in MATLAB by the stable Euler's implicit–explicit scheme, to calculate the principal coordinates $q_k(t)$, which are then multiplied by the corresponding plate modeshapes $\Phi_k(x,y)$ to generate the dynamic deflection $z(x,y,t)$. The static deflection of the plate, at each time step, under the same loading configuration, is calculated as a function of space and time. The ratio of the dynamic deflection to the corresponding static deflection, under the equivalent loading conditions, is defined as the dynamic load factor (DLF), i.e.,

$$\mathrm{DLF} \equiv \max\left[\frac{z(x,y,t)}{\max(z_{\mathrm{st}}(x,y,t))}\right]. \tag{14}$$

The static deflection is calculated by solving the following equation using Galerkin's method which includes the contribution of all the plate modeshapes. The classic static plate bending equation and the static deflection are

$$D\left(\frac{\partial^4 z(x,y,t)}{\partial x^4} + \frac{\partial^4 z(x,y,t)}{\partial x^2 \partial y^2} + \frac{\partial^4 z(x,y,t)}{\partial y^4}\right) = F(x,y,t);\ z_{\mathrm{st}}(x,y,t) = \sum_{j=1}^{\mathrm{mode}x} \sum_{l=1}^{\mathrm{mode}y} H_{jl} G_{jl}. \tag{15(a,b)}$$

Here, H_{jl} is the amplitude of the Galerkin's pre-multiplier $G_{jl}(x,y)$; and thus, it is the static counterpart of A_{jl}^k. The DLF varies as a function of the taxiing time, which has been non-dimensionalized as Non-D taxiing time $= \frac{t_{\mathrm{tax}}\omega_{n1}}{2\pi}$. Thus the DLF forms a very important design parameter for the structural designer, who does the static analysis of the corresponding area load only.

4 Results

4.1 Dry free vibration of the plate

The beam modeshapes are established for various end supports, which are used as admissible functions in the plate vibration analysis. The rigid body modes of heave, pitch, and roll become more prominent with decreasing $'k'$, and need to be included in the eigenvalue analysis. For the FF beam, the heave and pitch modeshapes are, respectively,

$$\phi_H(x) = 1; \phi_P(x) = 1 - \frac{2x}{L}, \tag{17(a,b)}$$

When $k \to 0$, $\phi_H(x)$, $\phi_P(x)$ are present, and when $k \to \infty$, they are absent. For all intermediate values of $'k'$, their prominence is inversely proportional to k. Suppose the above modeshapes are

$$\phi_H(x) = \exp\left[-\frac{kL^3}{EI}\right]; \phi_P(x) = \left(1 - \frac{2x}{L}\right)\exp\left[-\frac{kL^3}{EI}\right]. \tag{18}$$

Now $\exp[-k] = 1 - k + \frac{k^2}{2!} - \frac{k^3}{3!} + \cdots$ is a bounded function. Thus, $\exp\left[-\frac{kL^3}{EI}\right]$ is as a suitable coefficient for $\phi_H(x)$, $\phi_P(x)$.

Table 3 shows the first four frequency parameters βL of elastically supported beams, for a range of support factors $\frac{kL^3}{EI}$. For $\frac{kL^3}{EI} < 10^{-3}$, the βL values approach those of a FF beam, i.e., 4.73, 7.85. For $\frac{kL^3}{EI} > 10^6$, they approach those of a SS beam, i.e., $n\pi$. As seen in Fig. 4, the sharpest change in the *fundamental* βL occurs for $10^3 < \frac{kL^3}{EI} < 10^8$, which indicates the *transition zone* between the FF beam and the SS beam behaviors. However, for higher-order modes, this change occurs at the larger $\frac{kL^3}{EI}$ (Fig. 5). This has been explained by the authors in their previous work Datta and Thekinen 9]. The feasible eigenvector (among four) must be chosen to generate the correct modeshapes, which are listed in Table 4.

The fundamental modeshapes of elastically supported beams, for different $\frac{kL^3}{EI}$, are shown in Fig. 6. It may be observed that for small support factors ($\frac{kL^3}{EI} \to 0$), the fundamental mode tends to that of pure heave (zero curvature). On increasing $\frac{kL^3}{EI}$, the curvature of the modeshape increases and finally stabilizes to the first mode of a SS beam. The pitch mode of a FF beam (zero curvature) transforms to the second mode of a SS beam (Fig. 7). The third mode of the FF beam transforms into the third mode of the SS beam (Fig. 8).

Table 3 βL of elastically supported beam

$\frac{kL^3}{EI}$	βL_1	βL_2	βL_3	βL_4
0.00001	0.0669	0.0882	4.7300	7.8532
0.0001	0.1189	0.1565	4.7300	7.8532
0.001	0.2115	0.2783	4.7301	7.8532
0.01	0.3762	0.4949	4.7302	7.8532
0.1	0.6685	0.8801	4.7319	7.8536
1	1.1843	1.5642	4.7489	7.8573
10	2.0323	2.7666	4.9134	7.8947
100	2.8768	4.6638	6.0762	8.2754
1000	3.1111	6.0371	8.5656	10.6109
10,000	3.1385	6.2584	9.3399	12.3587
100,000	3.1413	6.2807	9.4164	12.5464
1,000,000	3.1416	6.2829	9.4239	12.5644
10,000,000	3.1416	6.2832	9.4247	12.5662

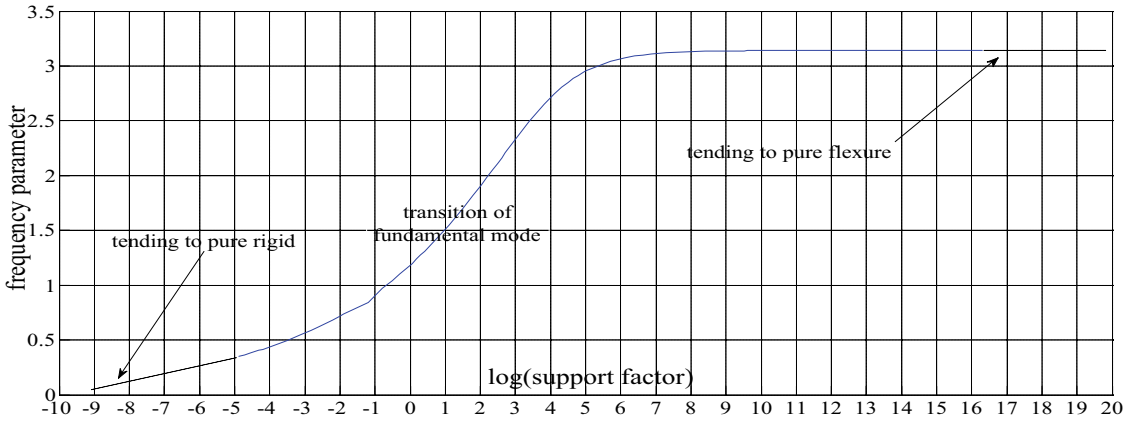

Fig. 4 Fundamental βL versus $\log_{10}\left[\frac{kL^3}{EI}\right]$

Fig. 5 First 8 frequency parameters βL versus $\log_{10}\left[\frac{kL^3}{EI}\right]$

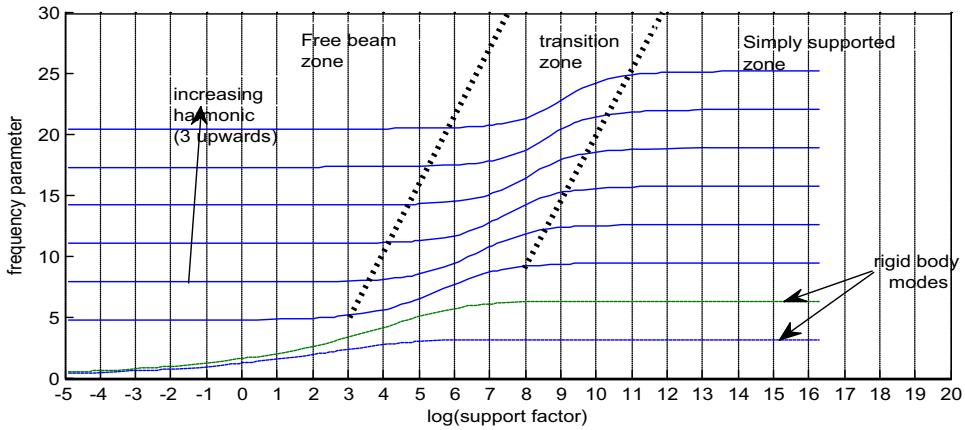

The beam modeshapes are used as admissible functions in the plate vibration. Galerkin's method is used to solve the eigenvalue problem, generating the eigenvalue (ω_k) and the eigenvectors $\left(A_{jl}^{k}\right)$. The middle-term of the biharmonic operator $\nabla^4\Phi(x,y)$, in the stiffness term causes the coupling between the beam modeshapes in the two perpendicular directions. It is only for the SSSS plate, that this biharmonic operator middle-term does not couple the beam modeshapes on either side, since the beam modeshapes and their curvatures are orthogonal to each other, and they drop out in the normal mode summation procedure.

Table 5 shows the first $3 \times 3 = 9$ natural frequencies of elastically supported square plates, for four different end support factors. The unique frequencies are in bold, while the repeated frequencies are in italics. For $\frac{kL^3}{EI} > 10^6$, the frequencies correspond to those of a SSSS plate, which has unique and repeated frequencies (identical twins). For $\frac{kL^3}{EI} < 10^{-3}$, they correspond to those of a FFFF plate, having unique, repeated, non-repeated frequencies (fraternal twins). This has been shown in Datta and Verma [7].

Figure 9 shows the first $7 \times 7 = 49$ modeshapes of a square plate, with an elastic support factor of 0.0001 and 1,000,000, respectively. The diagonal modeshapes correspond to the *unique frequencies* for mode index = 1, 4, 9, 16, 25, 36, 49. The first row/column stands for the *heave interaction* from one side with all other modes from the other side. The second row/column stands for the *pitch interaction* from one side with all other modes from the other side. The modeshape at positions (1,1), (1,2), and (2,1) are the pure rigid body modes. The modeshapes adjacent to the main diagonal are mirror images of each other, corresponding to the Identical twins. However, the alternate side-diagonal modes are very different from each other, though they have very close frequencies (Fraternal twins). Reducing the elastic support increases the prominence of the non-repeated frequency pairs.

Inclusion of the fluid inertia reduces the natural frequencies (Table 6a), making it more susceptible to transient impact loads. It is seen that the diagonal term A_{kk} is (much) larger than the non-diagonal terms A_{kn}. The NAVMI factor is directly proportional to the net volume

Table 4 Eigenvectors of the frequency equation

$\frac{kL^3}{EI}$	1,000,000	G1	G2	G3	G4
	Mode 1	0	1	0	0
	Mode 2	0	1	0	0
	Mode 3	0	1	0	0
Support	100	G1	G2	G3	G4
	Mode 1	0.1300	0.9761	0.1300	−0.1161
	Mode 2	−0.5034	−0.4795	−0.5034	0.5130
	Mode 3	−0.5752	0.06	−0.5752	0.5745
Support	10	G1	G2	G3	G4
	Mode 1	0.4387	0.7082	0.4387	−0.3371
	Mode 2	0.5486	−0.1041	0.5486	−0.6222
	Mode 3	−0.5243	0.4282	−0.5243	0.5166
Support	0.0001	G1	G2	G3	G4
	Mode 1	−0.7056	−0.0624	−0.7056	0.0216
	Mode 2	0.0552	−0.7035	0.0552	−0.7064
	Mode 3	−0.5044	0.4956	−0.5044	0.4956

enclosed by the modeshape. It also depends on the boundary conditions and the aspect ratio of the plate. The added mass associated with the fundamental modeshape is the highest, and it decreases with the higher-order modeshapes. This is because the volume enclosed under the 3-D plate modeshape decreases with higher modes. Also, the boundary conditions seem to have a less and less influence on the NAVMI magnitude with increasing modeshape index.

Since the mass matrix is diagonal and the added mass matrix is almost diagonal, the kth wet natural frequency is given as

$$\omega_{k,\text{wet}} = \omega_{k,\text{dry}}\sqrt{\frac{1}{1+A_{kk}/M_{kk}}}; M_{kk} = \int_0^L\int_0^B \Phi_k m \Phi_k \mathrm{d}x\mathrm{d}y; A_{kk} = \int_0^L\int_0^B \Phi_k \rho_{\text{water}} \Psi^* \mathrm{d}x\mathrm{d}y \tag{19}$$

5 Forced vibration

With the availability of the free vibration frequencies and modeshapes, the analysis proceeds to the forced vibration of the elastically supported floating plate, subject to the moving point load. Four different edge support factors have been used, i.e., $\frac{kL^3}{EI} = 0.0001, 10, 100, 10^6$. The flexural response has been studied for a wide range of non-D taxiing time, from 0.1 to 5. The normal mode summation method fails to decouple flexural degrees of freedom (except of SSSS plate), causing the necessity of matrix inversion in the time-integration of the coupled system of modal governing differential equations. Figure 10 shows the transient aircraft load, as a function of time, modeled as a point load moving across the plate in the x-direction, with the y-coordinate constant. The displacement has a parabolic relation with the taxiing time, as can be seen from the top view of the above diagram, with the locus of the aircraft following the white dotted line. The initial velocity of the craft is assumed to be 60 m/s, the taxiing distance is 90% of the length L, and the final velocity is zero, and hence the deceleration is computed as 2.25 m/s^2.

Figure 11 shows the DLF for a square plate, elastically supported with support factors of 1,000,000 (SSSS plate), 100, 10, and 1/10,000 (FFFF plate). Since small flexural amplitudes are assumed in the Kirchhoff's plate vibration,

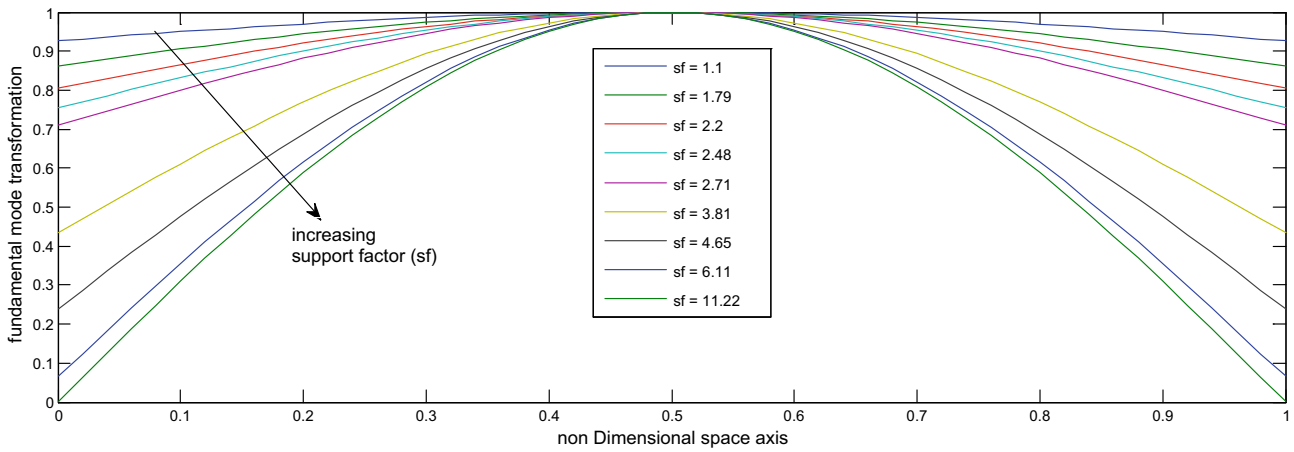

Fig. 6 Fundamental modeshapes of beam vibration with elastically supported ends, with various end supports

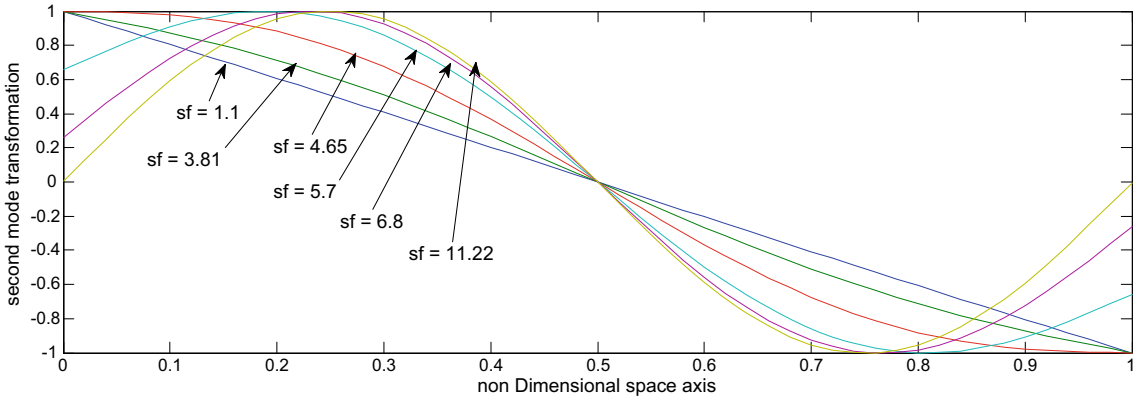

Fig. 7 Second modeshape (transition from pure rigid to completely flexure)

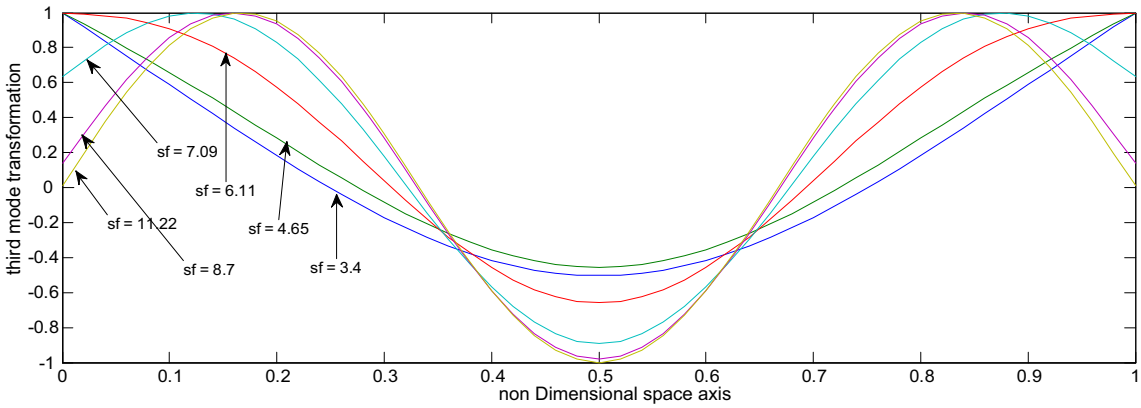

Fig. 8 Third modeshape transition for varying support factors

Table 5 First 3 × 3=9 non-D dry natural frequencies of a square plate with four different elastic support factors

k	1E + 06	Type	100	Type	10	Type	1E − 04	Type
1	**19.739**	**Unique**	**26.341**	**Unique**	**33.854**	**Unique**	**35.298**	**Unique**
2	*49.348*	*identical*	*67.678*	*identical*	*72.175*	*identical*	*72.535*	*identical*
3	*49.348*	*identical*	*67.678*	*identical*	*72.175*	*identical*	*72.535*	*identical*
4	**78.957**	**Unique**	**103.00**	**Unique**	**104.90**	**Unique**	**105.22**	**Unique**
5	*98.696*	*identical*	128.86	fraternal	130.07	fraternal	129.66	fraternal
6	*98.696*	*identical*	128.87	fraternal	133.53	fraternal	133.74	fraternal
7	*128.30*	*identical*	*160.11*	*identical*	*160.57*	*identical*	*160.67*	*identical*
8	*128.30*	*identical*	*160.11*	*identical*	*160.57*	*identical*	*160.67*	*identical*
9	**177.65**	**Unique**	**211.78**	**Unique**	**211.35**	**Unique**	**211.32**	**Unique**

the stresses are linearly proportional to the deflection. When the added mass is included in the forced vibration GDE, and the taxiing time is non-dimensionalized by the first wet flexural period of the plate, the wet DLF characteristics replicate the dry DLF [6]. The *three distinct zones* of the dynamic response are demarcated as follows:

- *Quasi-static zone* (non-D taxiing time >5) At larger taxiing time, the maximum dynamic deflection is only 5–10% greater than the maximum static deflection. Thus, the dynamic stresses developed due to the decelerating aircraft load, is 5–10% greater than that predicted through the static analysis.
- *Dynamic zone* (0.3 < non-D taxiing time < 3) At shorter taxiing time, the dynamic stress overshoots to 30–60% above the static stress. A non-D taxiing time $\approx$0.8, the DLF is $\approx$1.5 for a large range of support factors, even if the plate approaches FFFF.
- *Impulse zone* (non-D taxiing time <0.3) At very small taxiing time, the load moves across so fast that the structure does not get the time to respond, while the

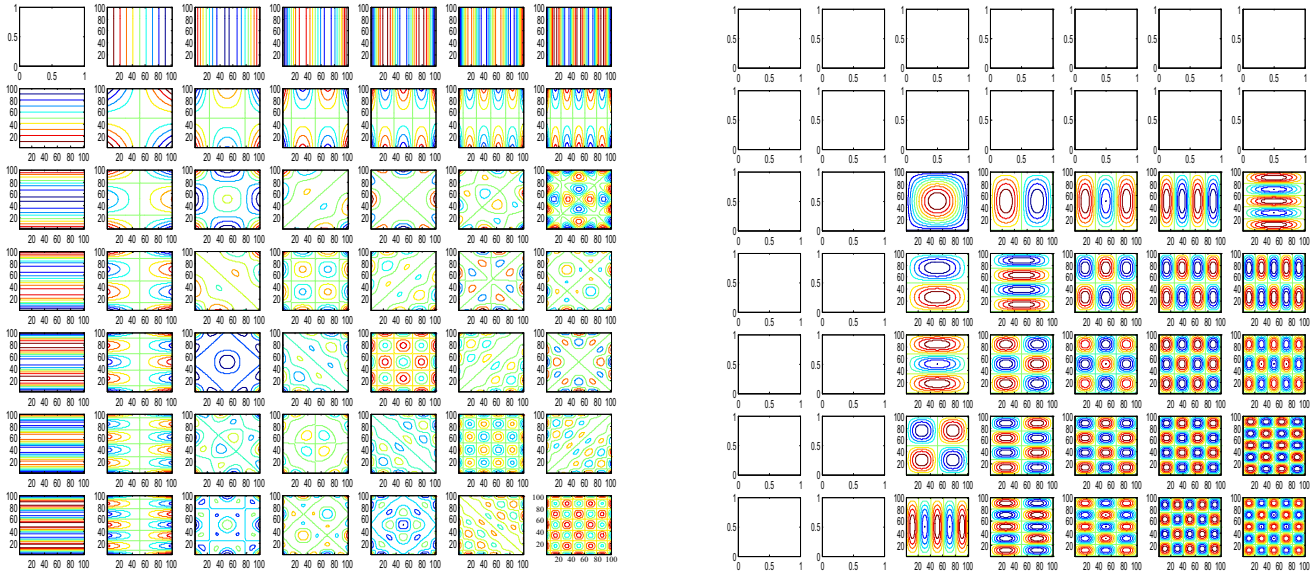

Fig. 9 First $7 \times 7 = 49$ modeshapes of a square plate with elastic support factor $\frac{kL^3}{EI}$ = 1/10,000, 1,000,000

Table 6 First $3 \times 3 = 9$ (a) non-D wet natural frequencies and (b) NAVMI factors of a square plate with four different $\frac{kL^3}{EI}$

$\frac{kL^3}{EI}$	1E + 06	100	10	1E − 04
(a)				
1	7.8282	12.039	24.480	26.017
2	26.829	45.074	54.289	55.030
3	26.829	45.074	54.289	55.030
4	47.795	76.596	81.142	81.671
5	59.688	93.722	102.50	102.85
6	62.070	93.962	102.63	103.16
7	84.358	124.61	127.28	127.56
8	84.358	124.61	127.28	127.56
9	122.98	169.88	170.52	170.58
(b)				
1	0.4104	0.2902	0.0696	0.0642
2	0.1825	0.0961	0.0576	0.0551
3	0.1825	0.0961	0.0576	0.0551
4	0.1324	0.0619	0.0514	0.0505
5	0.1328	0.0683	0.0477	0.0462
6	0.1170	0.0675	0.0481	0.0464
7	0.1006	0.0498	0.0455	0.0452
8	0.1006	0.0498	0.0455	0.0452
9	0.0832	0.0424	0.0425	0.0427

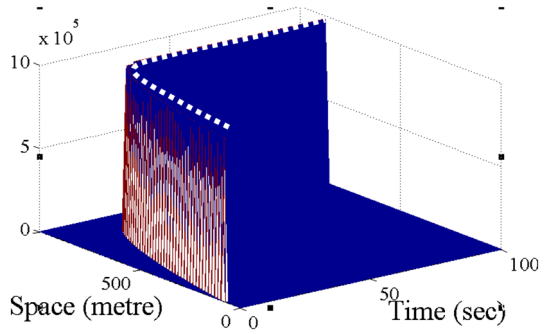

Fig. 10 Moving point load $F(x, B/2, t)$

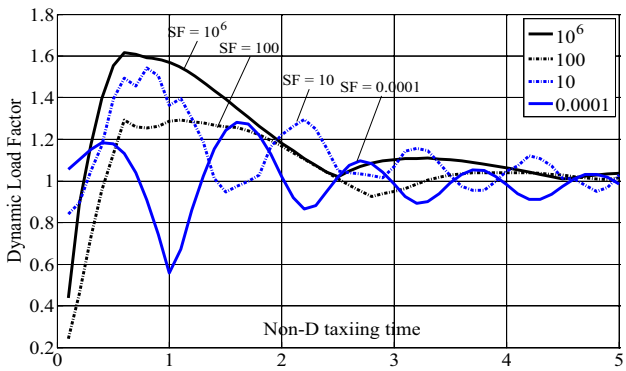

Fig. 11 DLF versus Non-D taxiing time for square plates with four different support factors (SF)

static analysis overpredicts the deflection due to a moving impulse function (Dirac Delta).

Since the change in the behavior from FFFF to SSSS plate is seen between support factors of 10 and 100, the nature of the DLF characteristics also changes between these two magnitudes of the support. The DLF of the SSSS plate may be verified from Datta [6]. As seen in Fig. 11, the DLF for support factor = 1,000,000 (SSSS) and 100 has somewhat similar trends. The peak DLF decreases with

decreasing elastic edge supports of the plate. Between support factor of 100 and 10, the plate behavior switches from a nearly SSSS plate to a nearly FFFF plate. In this zone, the DLF characteristics show more frequent oscillations over the same taxing time range, as seen for DLF of plates with support factor 10 and 0.0001. This is due to the larger prominence of the rigid body modes in the normal mode summation of the force vibration GDE. Rigid body motions (heave, pitch, roll) offset the flexural deflections under the same moving load, reducing the dynamic stresses. However, too little elastic support increases the 3° of rigid body motion, which adversely affects the performance of the floating airport, and leads to radiation waves (which erode the nearby shore and disturb the naval traffic in its vicinity). An optimized choice of the elastic support is necessary to avoid this.

6 Discussion and conclusion

A modal analysis of elastically supported square floating plates is presented. The dry vibration analysis has been done by the Galerkin's method, including the rigid body modeshapes. Wet vibration analysis has been done using the flexural modeshapes, to establish the wet natural frequencies. The various modeshapes with unique frequencies, identical twins, and fraternal twins have been established for different elastic supports. Wet vibration analysis, with water on one side of the plate, is used to generate the modal added masses. This is followed by the forced vibration analysis of a square plate. Dynamic loading factors of the flexural deflection are calculated for a range of taxiing time. Optimum support factor ranges are recommended, which causes lower dynamic stresses, without exciting too much of the rigid body degrees of freedom. A support factor of 1000, with a non-dimensional taxiing time of more than 4.5, is the most recommended.

6.1 Engineering decision

- It is safe to work in the quasi-static zone of the shock response spectrum, where the non-D taxiing time >2.5.
- Working at a support factor <100 causes the prominence of rigid body modes in the response, and hence it should be >100.
- Working at too high support factor increases the dynamic overshoot to $\sim 60\%$ in $0.5 <$ non-D taxiing time < 2. It is conducive to work in a support factor of <1000.
- If the non-D taxiing time is very less, i.e., <0.25, working at a low support factor of <0.0001, gives a DLF > 1. In such situations, a stiffer support factor of >10 gives a DLF < 1. However, such a situation of instantaneous stopping of the aircraft is usually not possible since the aircraft takes some time to decelerate and come to rest.

References

1. N.J. Robinson, S.C. Palmer, A modal analysis of a rectangular plate floating on an incompressible fluid. J. Sound Vib. **142**(3), 453–460 (1990)
2. H. Kagemoto, M. Fujino, M. Murai, Theoretical and experimental predictions of the hydroelastic response of a very large floating structure in waves. Appl. Ocean Res. **20**, 135–144 (1998)
3. H. Endo, The behavior of a VLFS and an airplane during takeoff/landing run in wave condition. Mar. Struct. **13**, 477–491 (2000)
4. H. Seto et al., Integrated hydrodynamic-structural analysis of VLFS. Mar. Struct. **18**, 181–200 (2005)
5. S.H. Hashemi et al., Vibration analysis of rectangular Mindlin's plates on elastic foundations and vertically in contact with stationary fluid by the Ritz method. Ocean Eng. **37**, 174–185 (2010)
6. N. Datta, Hydroelastic response of marine structures to impact-induced vibrations, Dissertation for Doctor of Philosophy, Naval Architecture and Marine Engineering, University of Michigan, Ann Arbor, 2010
7. N. Datta, Y. Verma, Accurate Eigenvector-based generation and computational insights of Mindlin's plate modeshapes for twin frequencies. Int. J. Mech. Sci. **123**, 64–73 (2017)
8. N. Datta, A.W. Troesch, Hydroelastic response of Kirchhoff plates to transient hydrodynamic impact loads. Mar. Syst. Ocean Technol. **7**(2), 77–94 (2012)
9. N. Datta, J.D. Thekinen, Wet vibration of axially loaded elastically supported plates to moving loads: aircraft landing on floating airports, 32nd International Conference on Ocean, Offshore and Arctic Engg, Nantes, 2013